Protein Cell 2011, 2(8): 631–646
DOI 10.1007/s13238-011-1081-7

Protein & Cell

RESEARCH ARTICLE

Quantitative proteomics analysis of parthenogenetically induced pluripotent stem cells

Zhe Hu[1], Lei Wang[1], Zhensheng Xie[2], Xinlei Zhang[3], Du Feng[1], Fang Wang[1], Bingfeng Zuo[1], Lingling Wang[1], Zhong Liu[1], Zhisheng Chen[1], Fuquan Yang[2] ✉, Lin Liu[1] ✉

[1] Department of Cell Biology and Genetics, Key Laboratory of Bioactive Materials of Ministry of Education, College of Life Sciences, Nankai University, Tianjin 300071, China
[2] Laboratory of Proteomics, Institute of Biophysics, Chinese Academy of Sciences, Beijing 100101, China
[3] Center for Computational and Systems Biology, Institute of Biophysics, Chinese Academy of Sciences, Beijing 100101, China
✉ Correspondence: liulin@nankai.edu.cn (L. Liu), fqyang@ibp.ac.cn (F. Yang)
Received July 1, 2011 Accepted July 30, 2011

ABSTRACT

Parthenogenetic embryonic stem (pES) cells isolated from parthenogenetic activation of oocytes and embryos, also called parthenogenetically induced pluripotent stem cells, exhibit pluripotency evidenced by both *in vitro* and *in vivo* differentiation potential. Differential proteomic analysis was performed using differential in-gel electrophoresis and isotope-coded affinity tag-based quantitative proteomics to investigate the molecular mechanisms underlying the developmental pluripotency of pES cells and to compare the protein expression of pES cells generated from either the *in vivo*-matured ovulated (IVO) oocytes or from the *in vitro*-matured (IVM) oocytes with that of fertilized embryonic stem (fES) cells derived from fertilized embryos. A total of 76 proteins were upregulated and 16 proteins were downregulated in the IVM pES cells, whereas 91 proteins were upregulated and 9 were downregulated in the IVO pES cells based on a minimal 1.5-fold change as the cutoff value. No distinct pathways were found in the differentially expressed proteins except for those involved in metabolism and physiological processes. Notably, no differences were found in the protein expression of imprinted genes between the pES and fES cells, suggesting that genomic imprinting can be corrected in the pES cells at least at the early passages. The germline competent IVM pES cells may be applicable for germ cell renewal in aging ovaries if oocytes are retrieved at a younger age.

KEYWORDS parthenogenetic embryonic stem cell, proteome, fluorescent two-dimensional difference in-gel electrophoresis, isotope-coded affinity tag

INTRODUCTION

Parthenogenetic embryos in mammals show extremely poor development of extraembryonic tissues (Monk, 1988) and die at mid-gestation, presumably because of aberrant genomic imprinting (Mann et al., 1990; Surani, 1998). However, parthenogenetic embryonic stem cells (pES) generated from parthenogenetic embryos developed from artificially activated oocytes can differentiate into all cell types *in vivo* and *in vitro* and develop into functional organs in the body (Chen et al., 2009). pES cells may provide a potential source of histocompatible pluripotent stem cells that are applicable in cell transplantation therapy for oocyte donors (Brevini and Gandolfi, 2008) while avoiding the creation of a competent live embryo.

pES cells have been created from parthenogenetic blastocysts of mice (Jiang et al., 2007; Kim et al., 2007), rabbits (Fang et al., 2006; Wang et al., 2007), non-human primates (Cibelli et al., 2002; Dighe et al., 2008), and humans (De Sousa and Wilmut, 2007; Mai et al., 2007). Interestingly, unlike IVO pES derived from IVO mature oocytes, IVM pES cells, which are generated from immature oocytes collected from adult mouse ovaries following *in vitro* maturation and artificial activation, exhibit increased pluripotency, as evidenced by the higher chimera production and greater

differentiation potential to the germline (Liu et al., 2011). However, the mechanisms underlying the pluripotency and regulation of IVM pES cells remain to be determined.

Several recent studies analyzed the expression and methylation of the imprinted genes of pES cells and found that these cells express paternally imprinted genes in a pattern similar to that of fertilized embryonic stem (fES) cells derived from fertilized embryos (Jiang et al., 2007; Horii et al., 2008; Li et al., 2009). Moreover, pES cells undergo hypomethylation during isolation and *in vitro* culture and passages that may underlie the reactivation of the paternally imprinted genes in pES cells (Li et al., 2009; Liu et al., 2011). Many of the regulatory steps, particularly those involved in cell proliferation, migration, and differentiation, depend on translation and posttranslational modifications of proteins (Levchenko et al., 2005). Proteomics has been applied to study changes in global protein expression (Nagano et al., 2005; Wang and Gao, 2005). Recently, a conventional two-dimensional gel electrophoretic (2-DE) method has been used to analyze the proteome of mouse embryonic stem cells derived from fertilized, parthenogenetic, and androgenetic blastocysts, and a number of proteins were found differentially expressed (Cui et al., 2011). In the current study, a comprehensive analysis of the proteomes of two types of new pES cell lines was performed. Differences in protein profiling between fES and pES cells were compared using two complementary quantitative proteomic approaches, namely, the two-dimensional differential in-gel electrophoresis (2D-DIGE) (Lyakhovich et al., 2007), and isotope-coded affinity tag (ICAT)-based proteomics (Aebersold et al., 2000).

RESULTS

Protein identification and quantification via DIGE

Proteins were extracted from IVO pES (C3 cell line), IVM pES (1116 cell line), and fES cells (F1 cell line) at passage 10, and 50 μg proteins from each sample was loaded and run in 2D gels in three replicates. The cell line 1116 is a pESC line (named IVM pESCs) from parthenogenetic embryos developed from the immature oocytes of adult mouse ovaries following IVM and artificial activation, and the F1 cell line is a normal ES cell line established from fertilized embryos (Liu et al., 2011). The separated proteins were analyzed using the DeCyder software. More than 1400 protein spots were detected and matched between the gels. Twelve proteins were found differentially expressed between the fES and IVM pES cells, whereas 39 proteins were differentially expressed between the fES and IVO pES cells, based on the up- or downregulation using the 1.5-fold cut-off (Fig. 1). After DIGE experiments, 1 mg protein sample was loaded onto a 2D gel and separated to obtain a sufficient quantity of proteins for further identification. A total of 28 distinguishable spots were selected from the 2D gel for excision and identification via matrix-assisted laser desorption/ionization time-of-flight mass spectrometry (MALDI-TOF MS) or liquid chromatography-tandem mass spectrometry (LC-MS/MS). Twenty-two proteins with at least two unique peptides matched to each protein and with a protein score above 60 were identified using the Mascot search engine. Each spot quantity was calculated using the DeCyder 2D Software V6.5 and the data were transformed into 3D images (Fig. 2). Among the identified proteins, seven were found downregulated in IVM pES and four in IVO pES, whereas two were upregulated in IVM pES and 17 in IVO pES. Spot 1152, which was identified as peroxiredoxin 4 (Prdx4), was altered in both pES types and demonstrated similar regulation patterns in the two cell types.

Protein identification and quantification via ICAT analysis

Two parallel ICAT experiments between fES and IVM pES and between fES and IVO pES cells were conducted. The two separate data sets generated were labeled ICAT1 (fES and IVM pES) and ICAT2 (fES and IVO pES). ICAT-labeled peptides (fES sample was labeled with $ICAT_{H\ (heavy)}$ and pES with $ICAT_{L\ (light)}$) were first concentrated via avidin affinity chromatography and then subjected to LC-MS/MS analysis and database searching. A total of 684 proteins with $ICAT_H$/$ICAT_L$ ratios ranging from 0.13 to 2.20 were identified in IVO pES, and 564 with $ICAT_H/ICAT_L$ ratios ranging from 0.17 to 2.88, with at least more than two unique peptides, were detected in IVM pES. The mass spectra of the ICAT-labeled peptide pairs are shown in Fig. 3A and 3B. CQHAAEIITDLLR, a unique peptide from the far upstream element (FUSE)-binding protein 1 (FBP1), was detected by MS and generated b and y ions after a collision-induced dissociation with an ICAT tag at the N-terminal. The molecular weight of each b ion in $ICAT_H$-labeled fES is 9 Da more than $ICAT_L$-labeled IVM pES, suggesting that the peptides were all labeled with the ICAT reagents.

A total of 76 proteins were upregulated and 10 proteins were downregulated in IVM pES (1116) compared to fES (F1) (Table 1), whereas 80 proteins were upregulated and 6 proteins were downregulated in IVO pES (C3) compared to fES (F1) (Table 2), based on the 1.5-fold cut-off. Notably, 63 proteins were commonly expressed in both types of pES cells and showed similar up or downregulated patterns. Three proteins, namely, caldesmon 1, hypothetical protein LOC433182 (GI:70794816), and unnamed protein (GI:74142393) were differentially expressed between IVM pES (1116) and fES (F1), whereas seven proteins, namely, Prdx4, FBP1, nuclear matrix protein SNEV, stomatin-like protein 2, and three unnamed proteins (GI:74204235, GI: 149266312, and GI: 74181760) were differentially expressed between IVO pES (C3) and fES (F1) and identified using both 2DE and ICAT methods (hypothetical proteins and unnamed protein products are not shown in Tables 1 and 2).

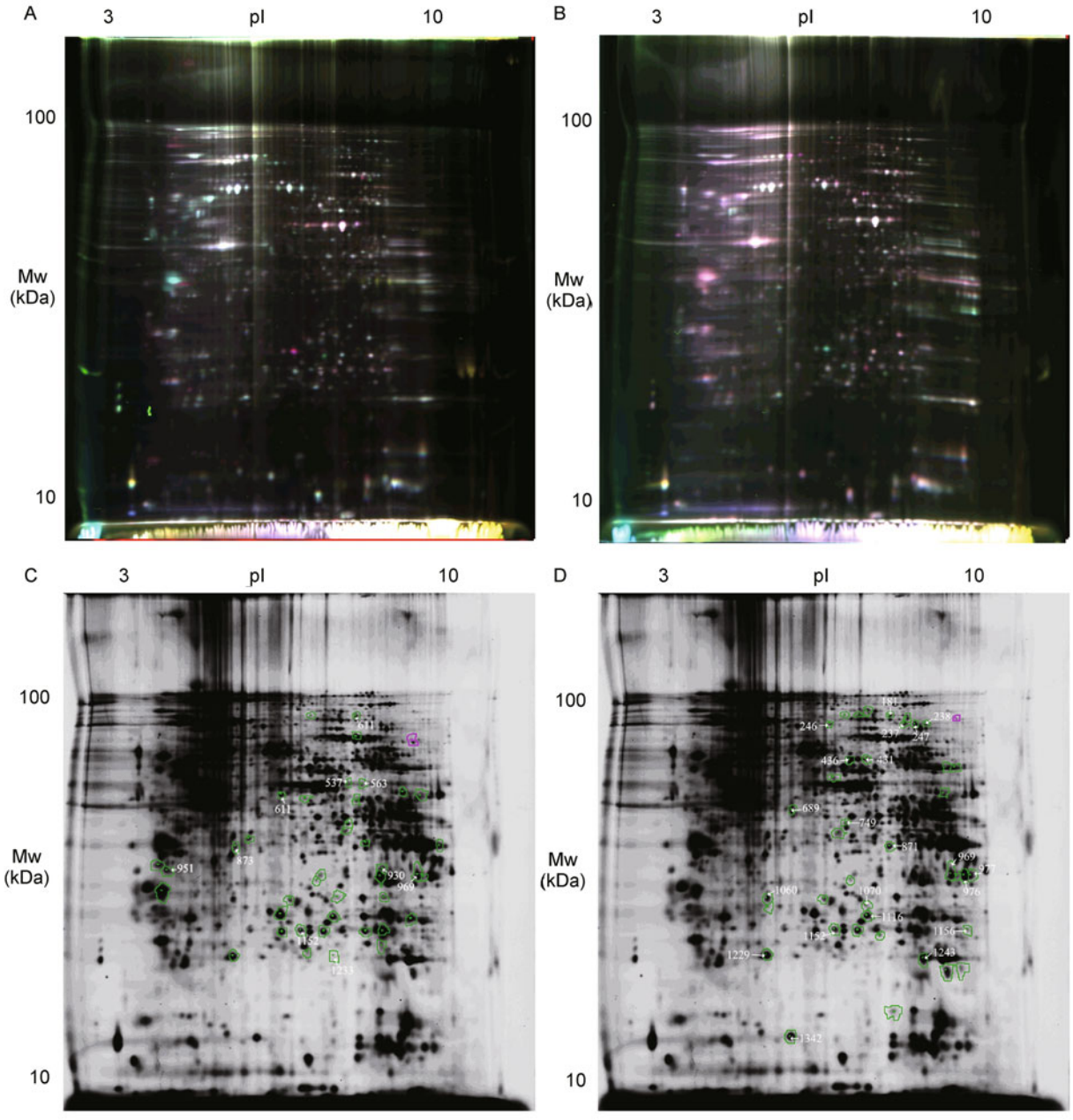

Figure 1. 2D DIGE analysis of the differentially expressed proteins between the pES and fES cells. (A) 2D DIGE comparison of proteins extracted from the IVM ES cells (Cy3, green) and those from fES cells (Cy5, red). (B) 2D DIGE comparison of proteins extracted from IVO ES cells (Cy3, green) and those from fES cells (Cy5, red). After the spots were determined using DeCyder and the difference between pES and fES was found statistically significant, a separate 2D gel loaded with 1 mg protein was run and stained with Coomassie brilliant blue. (C) Spots of differentially expressed proteins between fES and IVM pES were selected from separate 2D gels for peptide mass fingerprint analysis. (D) Spots of differentially expressed proteins between fES and IVO pES were selected from separate 2D gels for peptide mass fingerprint analysis. Each gel used pH 3–10 immobilized pH gradient (IPG) strips and the spots in the 10–100 kDa M_w range were separated.

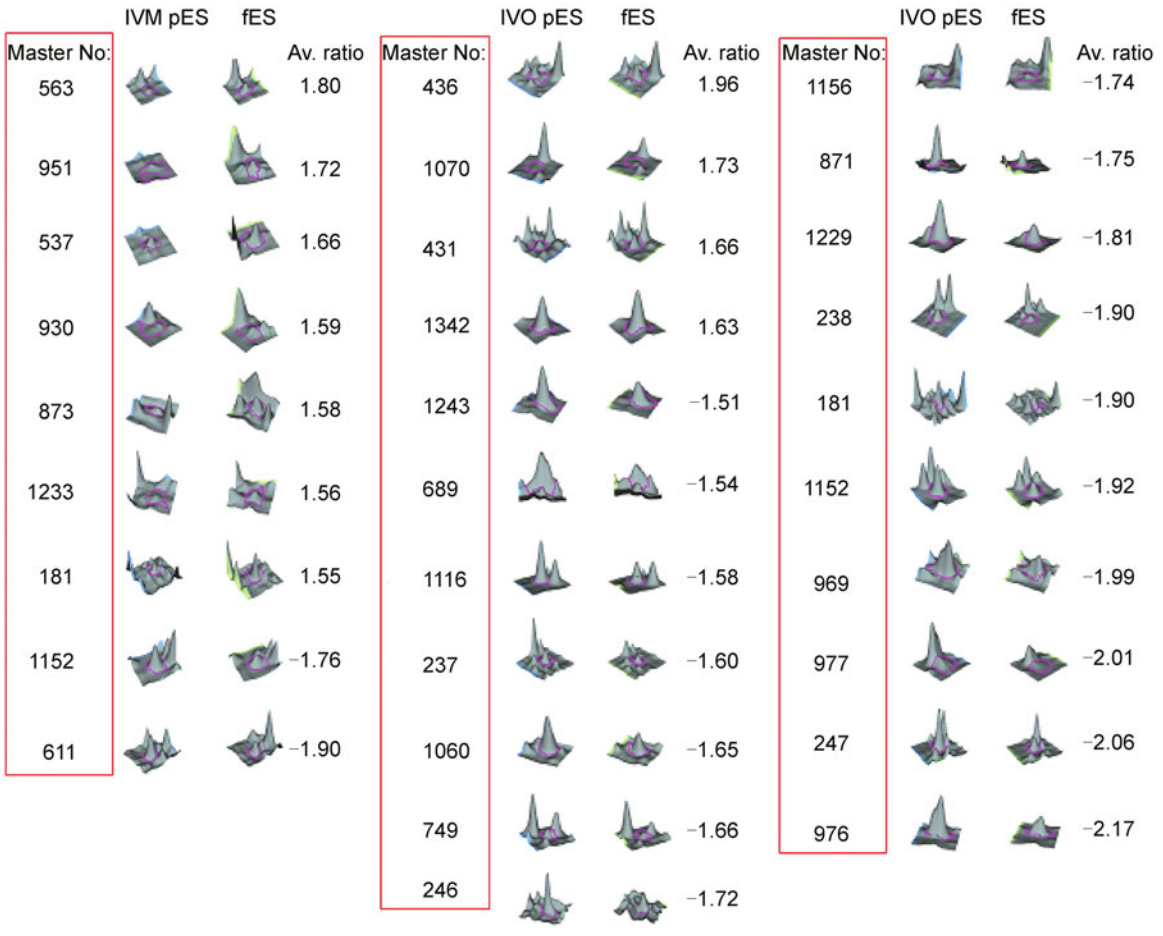

Figure 2. Correlation of the 3D images with the protein spots showing significant differences between fES and pES. Each differentially expressed spot between IVM pES and fES or IVO pES and fES is shown in 3D images. Spots enclosed in red lines represent the protein quantity. The average pES/fES ratios are also listed. The 3D images were directly exported using the DeCyder image analysis software. Master No. denotes the spot number annotated from the separate 2D gel. The fold differences for the spots shown have $p < 0.005$.

Verification via real-time polymerase chain reaction (PCR) analysis

The relative gene expression of 12 proteins that showed clear differences in expression, including some that were identified using both proteomic methods, was analyzed using real-time PCR and compared with that of fES cells, which served as controls because of the scarcity of specific antibodies for western blot verification. ICAT analysis results show that the protein levels of proteasome (prosome, macropain) activator subunit 4 (Psme4), deoxyuridine triphosphatase (Dut), polymerase (RNA) II (DNA-directed) polypeptide A (Polr2a), dihydrouridine synthase 3-like (Dus3l) in both pES, aquaporin 3 (Aqp3) in IVO pES, and spectrin beta 4 (Spnb4) in IVM pES showed over twofold increase compared with those of fES. Gene expression analysis shows that the genes for Psme4, Dut, Polr2a, Dus3l, and Aqp3 exhibited changes consistent with the protein variation detected using proteomics analysis; however, the Spnb4 in IVM pES was unchanged at the mRNA level and decreased in IVO pES cells (Fig. 4). The stomatin-like protein 2 (Stoml2), aldo-keto reductase family 1, member B3 (Akr1b3), protein arginine N-methyltransferase 7 (Prmt7), nuclear matrix protein SNEV (SNEV), FBP1 in IVO pES cells, and Prdx4 levels in both pES types were commonly elevated based on the DIGE results. Real-time PCR shows that only Prdx4 mRNA was unchanged in both pES cells as well as in the fES cells, but the other genes exhibited expression patterns similar to those of their protein expression (Fig. 4).

Localization and function annotation of differentially expressed proteins

The proteins were classified based on molecular functions and biological processes using the Panther Classification

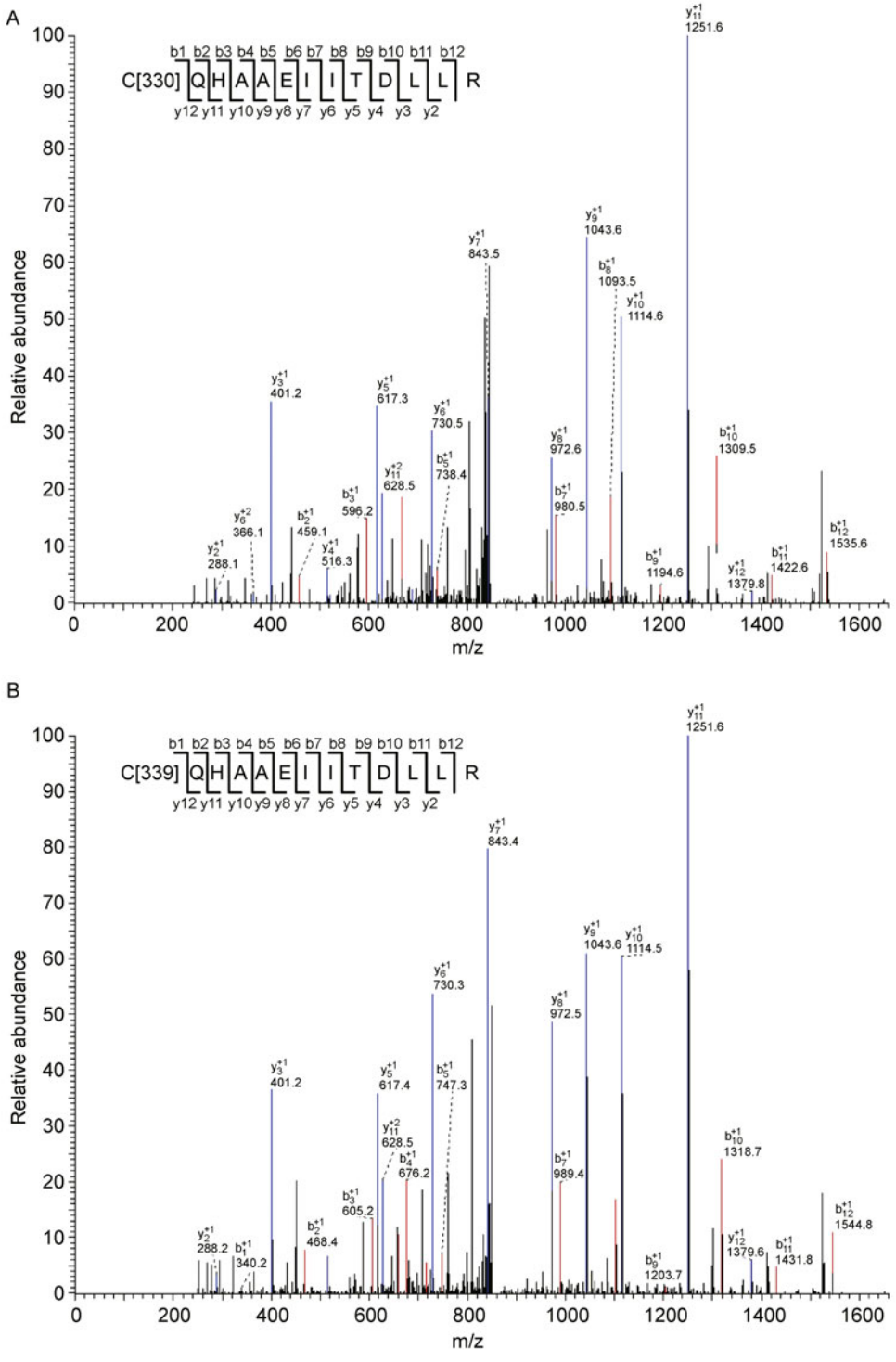

Figure 3. The ICAT sequence identification of the unique peptide QHAAEIITDLLR derived from FBP1. The peptides were labeled with an ICAT reagent containing a cysteine in the N-terminal. b and y ions were formed through a collision-induced dissociation. The spectrum is labeled with the b and y ions from the identified sequence (inset). (A) MS/MS spectra show peptides labeled with the light ICAT ($ICAT_L$) reagent. (B) MS/MS spectra show peptides labeled with the heavy ICAT ($ICAT_H$) reagent. The ICAT modification remained fairly stable and attached to the cysteine residue.

Table 1 Identification of differentially expressed proteins between fES and IVM pES

Note	Protein	Unique peptides	Total peptides	Description	Peptide sequence	Av ratio
#	gi|7949018|	2	3	Cell division cycle 37 homolog	KVAEC*QR	0.17
#	gi|6678656|	6	10	Laminin, alpha 1	C*SAGYHGNPR	0.24
#	gi|40254181|	1	1	Serine/threonine kinase 11 interacting protein	NC*ISATEEEVTPQHR	0.28
	gi|7709984|	2	3	Aquaporin 3	C*GEMLHIR	0.29
	gi|40556272|	1	3	Proteasome (prosome, macropain) activator subunit 4	C*VAEIIAGLIR	0.32
	gi|6677795|	1	1	Polymerase (RNA) II (DNA directed) polypeptide A	LTHVYDLC*K	0.44
#	gi|34147302|	1	2	TAFA3 protein	C*SC*LSGQVAGTTR	0.45
	gi|13928670|	8	21	Vacuolar protein sorting 35	AC*AELHQNVNVK	0.47
	gi|21450077|	2	4	Dihydrouridine synthase 3-like	C*VLFETFGR	0.47
	gi|6680027|	1	2	Glutamate dehydrogenase 1	C*AVVDVPFGGAK	0.49
	gi|57222238|	1	1	Maternal G10 transcript	IIEC*THC*GC*R	0.49
	gi|22203755|	5	8	Eukaryotic translation initiation factor 3, subunit 8	C*LEEFELLGK	0.5
	gi|19527174|	2	7	Splicing factor 3b, subunit 3	SEHPPLC*GR	0.5
	gi|21426821|	1	2	Ribosomal protein S28	TGSQGQC*TQVR	0.51
#	gi|21312422|	1	1	Mak3p homolog	LYIMTLGC*LAPYR	0.51
	gi|6680019|	3	10	Glutamate-cysteine ligase, modifier subunit	C*PSTHSEELR	0.52
	gi|20070408|	2	5	Glycine decarboxylase	C*HPQTIAVVQTR	0.52
	gi|6754620|	1	1	Mannosidase, alpha, class 1A, member 2	TC*HESYDR	0.53
	gi|31982367|	2	5	Faciogenital dysplasia homolog	VC*TDC*YVALHGAPGS-SPAC*SQHTPQR	0.54
	gi|21630283|	3	5	2'–5' oligoadenylate synthetase 1A	C*FQGAAHPVR	0.55
	gi|6678077|	4	7	Secreted acidic cysteine rich glycoprotein	APLIPMEHC*TTR	0.56
	gi|33859528|	3	7	Procollagen, type IV, alpha 1	AHGQDLGTAGSC*LR	0.57
	gi|9055370|	2	6	Eukaryotic translation initiation factor 3, subunit 2 (beta)	HVLTGSADNSC*R	0.57
	gi|58037335|	1	2	Developmental pluripotency-associated 2	WC*VVHGR	0.58
	gi|7305575|	2	3	Translocase of inner mitochondrial membrane 13 homolog a	MTSAC*HR	0.58
	gi|9845253|	3	4	Heterogeneous nuclear ribonucleoprotein H2	DLNYC*FSGMSDHR	0.58
	gi|31981382|	4	9	Inosine 5'-phosphate dehydrogenase 2	HGFC*GIPITDTGR	0.58
#	gi|27370520|	2	3	BPY2 interacting protein 1	STSPHDVDLC*LVSPC*EF-SHR	0.58
	gi|31560618|	3	6	Budding uninhibited by benzimidazoles 3 homolog	LC*QFHR	0.59
#	gi|85701844|	1	1	Zinc finger protein 568	QAAVTSVERPDSVQC*-TAHR	0.59
#	gi|30102930|	2	4	PWP2 periodic tryptophan protein homolog	C*GNLNFTHDGNSVISPV-GNR	0.59
	gi|21281687|	1	2	Deoxyuridine triphosphatase	IAQLIC*ER	0.6

(*Continued*)

Note	Protein	Unique peptides	Total peptides	Description	Peptide sequence	Av ratio
	gi|31791057|	12	28	Laminin, gamma 1	DNTAGPHC*EK	0.6
	gi|11612505|	2	5	Stromal cell-derived factor 2-like 1	C*SGQHWER	0.6
	gi|31541819|	1	2	Ras-related GTP binding A	LSRPLEC*AC*FR	0.6
	gi|13937395|	6	12	Arsenate resistance protein 2	C*GIIHVR	0.6
	gi|16418339|	11	51	Ribosomal protein 10	M[147]LSC*AGADR	0.6
#	gi|40556384|	2	2	PHD zinc finger protein Jade1	C*IHASSTISR	0.6
	gi|31559817|	2	3	Topoisomerase (DNA) II beta binding protein	SSVSHC*ILDDSTVR	0.61
	gi|31982373|	3	8	Fibrillarin	HEGVFIC*R	0.61
#	gi|21704156|	1	2	Caldesmon 1	C*LATLSQIAYQR	0.62
	gi|21704144|	3	12	Methionine adenosyltransferase II, alpha	TC*NVLVALEQQSPDIAQ-GVHLDR	0.62
#	gi|31981842|	4	11	3-hydroxy-3-methylglutaryl-Coenzyme A synthase 1	HSLSYDC*IGR	0.62
	gi|6678483|	5	14	Ubiquitin-activating enzyme E1, Chr X	VGEFC*HSR	0.63
	gi|21703808|	3	4	Protein arginine N-methyltransferase 7	QVSSSAAC*HSR	0.63
#	gi|7710040|	1	2	Inner centromere protein	IIC*HSYLER	0.63
	gi|83816893|	5	12	DEAD (Asp-Glu-Ala-Asp) box polypeptide 5	ELAQQVQQVAAEYC*R	0.63
	gi|39930325|	1	1	Kinesin-like 7	C*FGETLSTLNFAQR	0.63
	gi|10946928|	12	35	Heterogeneous nuclear ribonucleoprotein H1	DLNYC*FSGMSDHR	0.63
	gi|6671561|	6	13	Adaptor protein complex AP-2, alpha 1 subunit	AC*NQLGQFLQHR	0.63
	gi|12963691|	2	3	Tubulointerstitial nephritis antigen-like	C*MMHSR	0.635
#	gi|58037197|	1	2	Zinc finger, HIT domain containing 1	C*LGTHQETR	0.64
	gi|6754854|	10	19	Nidogen 1	C*EC*VEGYHFSDR	0.64
	gi|50234896|	2	5	Ubiquitin-conjugating enzyme E2O	LGC*FDHAQR	0.64
	gi|7949012|	3	9	Nedd8 ultimate buster-1	AC*DGNVDHAATHISNR	0.64
	gi|7949035|	2	6	Dimethylarginine dimethylaminohydrolase 2	C*SHALIR	0.64
	gi|34328204|	5	11	Valyl-trna synthetase 2	C*SIHLQLQGLVDPAR	0.64
#	gi|51491860|	3	4	Ubiquitin specific protease 7	HGC*VR	0.64
	gi|6677769|	7	35	Ribosomal protein L12	C*TGGEVGATSALAPK	0.645
	gi|77736535|	1	3	Syntaxin 18	TC*SEAIHQLR	0.65
	gi|6997239|	2	4	Poly(rc) binding protein 2	AITIAGIPQSIIEC*VK	0.65
#	gi|31982762|	1	3	KH domain containing, RNA binding, signal transduction associated 1	SC*SKDPSGAHPSVR	0.65
	gi|6671509|	17	69	Actin, beta, cytoplasmic	C*PEALFQPSFLGMESC*-GIHETTFNSIMK	0.65
#	gi|42476274|	2	4	X-prolyl aminopeptidase (aminopeptidase P) 1, soluble	NSEYVAEPIQAYIIPSG-DAHQSEYIAPC*DC*RR	0.66
	gi|29789343|	7	19	Eukaryotic translation initiation factor 3, subunit 9	FSHQGVQLIDFSPC*ER	0.66
#	gi|21704248|	1	2	U3 snornp-associated protein	LWQC*GEGFR	0.66

(*Continued*)

Note	Protein	Unique peptides	Total peptides	Description	Peptide sequence	Av ratio
	gi|31982186|	1	2	Malate dehydrogenase 2, NAD (mitochondrial)	GC*DVVVIPAGVPR	0.66
	gi|28076873|	5	15	Coiled-coil-helix-coiled-coil-helix domain containing 5	C*TSSHPIIR	0.66
	gi|6678515|	8	11	Uridine phosphorylase 1	FVC*VGGSSSR	0.66
#	gi|46877109|	2	3	UDP-N-acetyl-alpha-D-galactosamine:polypeptide N-acetylgalactosaminyltransferase 2	HDQC*QR	0.66
	gi|12963757|	3	12	Myo-inositol 1-phosphate synthase A1	SC*IENIFR	0.67
	gi|46849812|	35	110	Fibronectin 1	C*DPHEATC*YDDGK	0.67
	gi|19527048|	12	45	Heterogeneous nuclear ribonucleoprotein F	DLSYC*LSGMYDHR	0.67
	gi|9507023|	1	1	Rab geranylgeranyl transferase, a subunit	SC*LLPQLHPQPDSG-PQGR	0.67
	gi|40254525|	2	3	Tropomyosin 3, gamma	EEHLC*TQR	0.67
#	gi|6679110|	3	6	Nucleoplasmin 3	VPAPVTMDSFFFGC*ELS-GHTR	0.67
	gi|6754544|	2	2	Ligase I, DNA, ATP-dependent	C*ADLSLSPIYPAAR	1.5
#	gi|12963491|	1	1	Enolase 1, alpha non-neuron	FGANAILGVSLAVC*K	1.5
#	gi|8394239|	1	2	Squamous cell carcinoma antigen recognized by T-cells 3	AHGDTQHC*R	1.65
	gi|70887769|	1	2	Metal response element binding transcription factor 2	HC*GLSDSR	1.7
	gi|33859506|	7	26	Albumin 1	EC*C*HGDLLEC*ADDR	1.8
	gi|77377292|	1	3	Sulfatase modifying factor 2	C*ASSAGRPK	1.85
	gi|6680353|	2	3	Interferon activated gene 202B	IC*DLHLQTEER	1.87
	gi|6680952|	3	4	Calponin 2	C*ASQVGM[147]TAPGTR	1.87
#	gi|6679651|	8	50	Enolase 3, beta muscle	FGANAILGVSLAVC*K	2
#	gi|30794220|	1	2	Spectrin beta 4	SC*QDHLNSR	2.88

Specifically expressed in IVM pES; Those without # were commonly expressed in both IVM pES and IVO pES cells.

Table 2 Identification of differentially expressed proteins between fES and IVO pES

Note	Protein	Unique peptides	Total peptides	Description	Peptide sequence	Av ratio
	gi|12963663|	1	1	Magnesium-dependent phosphatase-1	LFQQILSGVDYC*HR	0.13
	gi|40556272|	1	2	Proteasome (prosome, macropain) activator subunit 4	C*ASQAGMTAYGTR	0.2
	gi|45544618|	5	12	Methylthioadenosine phosphorylase	TSLRPQTFYDGSHC*SAR	0.28
	gi|21426821|	1	2	Ribosomal protein S28	YSSLYAQLC*LR	0.32
	gi|7709984|	2	3	Aquaporin 3	C*GEMLHIR	0.36
#	gi|13385998|	1	1	TNF receptor-associated protein 1	NIYYLC*APNR	0.36
	gi|22203755|	4	7	Eukaryotic translation initiation factor 3, subunit 8	C*HAPLAQAQALVTSELER	0.38
	gi|6680027|	1	2	Glutamate dehydrogenase 1	SNPVPILIPC*HR	0.39
	gi|58037335|	1	2	Developmental pluripotency-associated 2	ALHEQEIDC*QLVEAVDGK	0.39

(*Continued*)

Note	Protein	Unique peptides	Total peptides	Description	Peptide sequence	Av ratio
	gi|19527028|	1	2	High density lipoprotein binding protein	AQIEQVIANC*EHK	0.42
	gi|13937395|	4	5	Arsenate resistance protein 2	C*GIIHVR	0.43
	gi|12963757|	2	4	Myo-inositol 1-phosphate synthase A1	SC*IENIFR	0.44
	gi|11612505|	2	3	Stromal cell-derived factor 2-like 1	C*SGQHWER	0.44
	gi|6677795|	1	1	Polymerase (RNA) II (DNA directed) polypeptide A	LTHVYDLC*K	0.44
	gi|31981382|	2	2	Inosine 5'-phosphate dehydrogenase 2	HGFC*GIPITDTGR	0.44
	gi|6680019|	2	4	Glutamate-cysteine ligase, modifier subunit	C*PSTHSEELR	0.44
	gi|31982367|	1	2	Faciogenital dysplasia homolog	KTSDFNTFLAQEGC*TR	0.45
	gi|21281687|	1	2	Deoxyuridine triphosphatase	VC*ENIPIVLC*GNK	0.47
	gi|50234896|	1	2	Ubiquitin-conjugating enzyme E2O	HYPLNTVTFC*DLDPQER	0.47
	gi|21450077|	2	4	Dihydrouridine synthase 3-like	C*VLFETFGR	0.47
	gi|6680193|	2	3	Histone deacetylase 1	ISIC*SSDKR	0.49
	gi|7305575|	2	2	Translocase of inner mitochondrial membrane 13 homolog a	MTSAC*HR	0.49
	gi|34328204|	4	5	Valyl-trna synthetase 2	C*VVHPFLSR	0.49
#	gi|6678419|	1	2	Tripeptidyl peptidase II	ASYPC*MSLHGGIDQYDR	0.49
	gi|46849812|	29	71	Fibronectin 1	C*DPHEATC*YDDGK	0.5
#	gi|19923052|	1	1	Acyl-Coa thioesterase 7	YFC*HC*C*SVEIVPR	0.51
	gi|6678483|	5	8	Ubiquitin-activating enzyme E1, Chr X	YFLVGAGAIGC*ELLK	0.54
	gi|28916693|	6	14	Gelsolin	LFAC*SNR	0.55
	gi|21630283|	3	5	2'–5' oligoadenylate synthetase 1A	C*FQGAAHPVR	0.55
	gi|37674224|	1	1	Guanine nucleotide binding protein-like 3 (nucleolar)-like	FAC*NTC*PYVHNITR	0.55
#	gi|7948999|	5	10	Peroxiredoxin 4	ENEC*HFYAGGQVYP-GEASR	0.55
	gi|9845253|	3	4	Heterogeneous nuclear ribonucleoprotein H2	DLNYC*FSGMSDHR	0.55
	gi|28076873|	3	6	Coiled-coil-helix-coiled-coil-helix domain containing 5	C*TSSHPIIR	0.55
#	gi|6755100|	7	8	Proliferation-associated 2G4	AAHLC*AEAALR	0.55
	gi|57222238|	1	1	Maternal G10 transcript	RGFC*FITYTDEEPVK	0.56
	gi|13385958|	2	3	Ribosomal protein S27-like	LTEGC*SFR	0.57
	gi|40556608|	21	94	Heat shock protein 1, beta	C*LELFSELAEDK	0.57
	gi|31541819|	1	2	Ras-related GTP binding A	VTVFQYIGELC*R	0.57
	gi|28269697|	5	8	NMDA receptor-regulated gene 1	EALEHLC*TYEK	0.58
#	gi|6754474|	1	1	Karyopherin (importin) alpha 2	ATHDGSSC*GDDR	0.58
	gi|29789343|	6	12	Eukaryotic translation initiation factor 3, subunit 9	FSHQGVQLIDFSPC*ER	0.58
	gi|12963691|	2	2	Tubulointerstitial nephritis antigen-like	C*LEEFELLGK	0.58
	gi|21703808|	1	2	Protein arginine N-methyltransferase 7	EC*LPLAIFLR	0.59

(*Continued*)

Note	Protein	Unique peptides	Total peptides	Description	Peptide sequence	Av ratio
	gi|13384718|	2	11	Ubiquitin-conjugating enzyme E2D 3 (UBC4/5 homolog, yeast)	IYHPNINSNGSIC*LDILR	0.59
#	gi|12331400|	2	4	Acyl-Coenzyme A thioesterase 3, mitochondrial	SLDIC*HPQER	0.6
#	gi|31982690|	1	2	Epidermal growth factor-containing fibulin-like extracellular matrix protein 2	LYSEEKPQEAVPHLEAAL-QEYFVADEEC*R	0.6
	gi|6755210|	1	2	Proteasome 26S non-ATPase subunit 13	LERPIHLAC*TAGIFDPYV-PPEGDAR	0.6
#	gi|40254375|	1	2	L-threonine dehydrogenase	NPAPDLC*IQRPR	0.6
	gi|21539599|	5	13	Ubiquinol-cytochrome c reductase hinge protein	SQTEEDC*TEELFDFLHAR	0.61
	gi|6754854|	8	13	Nidogen 1	C*EC*VEGYHFSDR	0.61
	gi|77736535|	1	1	Syntaxin 18	C*YDIIPDTLLELGEIPTLK	0.61
	gi|22165384|	6	18	Tubulin, beta, 2	LTTPTYGDLNHLVSATMS-GVTTC*LR	0.61
	gi|31559817|	1	2	Topoisomerase (DNA) II beta binding protein	C*VHLR	0.62
	gi|20070408|	2	3	Glycine decarboxylase	C*HPQTIAVVQTR	0.62
	gi|39930325|	1	1	Kinesin-like 7	DTEQYEHEDFLIKPTDN-LIVC*GR	0.62
	gi|6678077|	3	4	Secreted acidic cysteine rich glycoprotein	LHLDYIGPC*K	0.63
	gi|9055214|	5	10	Eukaryotic translation initiation factor 3, subunit 7 (zeta)	NLAMEATYINHNF-SQQC*LR	0.63
	gi|31560618|	3	4	Budding uninhibited by benzimidazoles 3 homolog	LC*QFHR	0.63
#	gi|12584986|	3	7	Ribosomal protein L23	ISLGLPVGAVINC*ADNT-GAK	0.635
	gi|21704144|	2	7	Methionine adenosyltransferase II, alpha	TC*NVLVALEQQSPDIA-QGVHLDR	0.64
	gi|31982373|	3	5	Fibrillarin	HEGVFIC*R	0.64
	gi|28077103|	2	3	Phospholipase A2, activating protein	LSC*SLPGHELDVR	0.64
	gi|7949012|	2	4	Nedd8 ultimate buster-1	AC*DGNVDHAATHISNR	0.64
#	gi|6679759|	27	43	Fibrillin 1	C*IC*KPGFQLASDGR	0.64
#	gi|12963591|	3	5	Stomatin-like protein 2	ESLNANIVDAINQAADC*-WGIR	0.64
	gi|39652626|	1	2	Bisphosphate 3'-nucleotidase 1	C*SWLVVQC*LLR	0.64
	gi|16418339|	11	32	Ribosomal protein 10	M[147]LSC*AGADR	0.65
#	gi|84662730|	2	4	Far upstream element (FUSE) binding protein 1	C*QHAAEIITDLLR	0.65
	gi|19527358|	6	9	Nuclear matrix protein SNEV	QELSHALYQHDAAC*R	0.65
#	gi|94369185|	5	12	PREDICTED: similar to phosphoglycerate mutase 1 (Phosphoglycerate mutase isozyme B) (PGAM-B) (BPG-dependent PGAM 1)	YADLTEDQLPSC*ESLKD-TIAR	0.65
	gi|40254646|	8	14	Adaptor protein complex AP-2, alpha 2 subunit	AC*NQLGQFLQHR	0.65

(*Continued*)

Note	Protein	Unique peptides	Total peptides	Description	Peptide sequence	Av ratio
	gi|31542192|	1	1	Proline arginine rich coiled coil 1	AC*QVAHC*ASSR	0.65
	gi|33859528|	1	2	Procollagen, type IV, alpha 1	ATPPQIVNGNHYC*GDYE-LFVEAVEQDTLQEFLK	0.66
#	gi|21312314|	1	1	Dual specificity phosphatase 3 (vaccinia virus phosphatase VH1-related)	VLVHC*R	0.66
	gi|6997239|	2	4	Poly(rc) binding protein 2	INISEGNC*PER	0.67
	gi|23956066|	2	5	Gamma isoform of regulatory subunit B56, protein phosphatase 2A	C*VSSPHFQVAER	0.67
#	gi|34328173|	1	2	Farnesyl diphosphate farnesyl transferase 1	C*SDFTEEIC*R	0.67
	gi|50511310|	1	2	Coactivator-associated arginine methyltransferase 1	AASPQDLAGGYTSS-LAC*HR	0.67
#	gi|13385408|	6	10	Ribosomal protein L11	IAVHC*TVR	0.67
	gi|33859506|	6	14	Albumin 1	EC*C*HGDLLEC*ADDR	1.84
	gi|6754544|	1	1	Ligase I, DNA, ATP-dependent	HEC*AEALGAIAR	1.85
	gi|6680353|	2	3	Interferon activated gene 202B	IC*DLHLQTEER	1.87
	gi|6680952|	3	4	Calponin 2	C*ASQVGM[147]TAPGTR	1.87
	gi|77377292|	1	2	Sulfatase modifying factor 2	LNAIC*AQVIPFLSQEHQQ-QVVQAVER	2.00
	gi|70887769|	1	2	Metal response element binding transcription factor 2	HC*GLSDSR	2.20

Specifically expressed in IVO pES; Those without # were commonly expressed in both IVM pES and IVO pES cells.

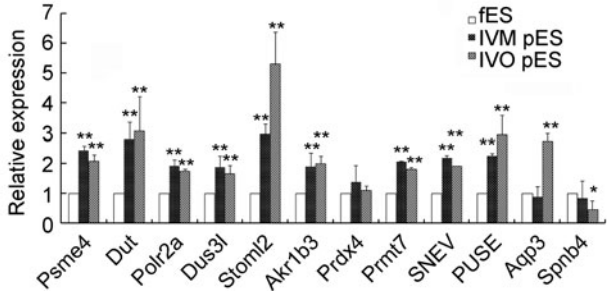

Figure 4. Relative mRNA expression levels of selected genes in IVO pES and IVM pES cells compared with those of fES as detected by real-time PCR analysis. GAPDH served as the internal control. Bars indicate mean + SEM ($n = 3$). *$p < 0.05$; **$p < 0.01$ *vs* fES cells.

System (www.pantherdb.org), which reveal that the binding and transcription activities are the main functions of the differentially expressed proteins in both pES cell types.

Many differentially expressed proteins that were elevated in both IVO and IVM pES are involved in cellular metabolism, protein metabolism, cytoplasm organization and biogenesis, and ribosome biogenesis and assembly, and the variation showed similar patterns. No distinct signaling pathways for the preferentially expressed proteins in the pES cells were found, except for those of mitogen-activated protein kinase (MAPK) 4 (MAPK pathway) and catenin (Wnt signaling pathway); the MAPK 4 and catenin levels were increased in both types of pES cells. In addition, arginine N-methyltransferase 7 and histone deacetylase 1, which are involved in histone methylation and acetylation, respectively, showed higher expression levels in pES cells than in fES cells (Tables 1 and 2). No imprinted genes were upregulated in pES cells, except for the paternally expressed imprinted gene Impact (imprinted and ancient), which was detected via MS and whose unique STFQAHVAPVVCPEQVK peptide was detected in the ICAT experiment. The protein Impact was slightly downregulated in IVO and IVM pES compared to fES, with an average ratio of 0.80 and 0.85, respectively.

Ontological analysis shows that proteins for RNA processing, rRNA metabolism, processing and transcription, biopolymer metabolism, cell organization and biogenesis, and endoderm development were enriched in IVM pES cells (Fig. 5). The levels of proteins involved in biosynthesis, carboxylic acid metabolism, cellular macromolecular metabolism, organic acid metabolism, nitric oxide biosynthesis, nitric oxide metabolism, nitrogen compound metabolism, nitric oxide biosynthesis, protein complex localization, and serine family amino acid metabolism varied in IVO pES cells. Notably, nestin and BPY2-interacting protein 1, which are

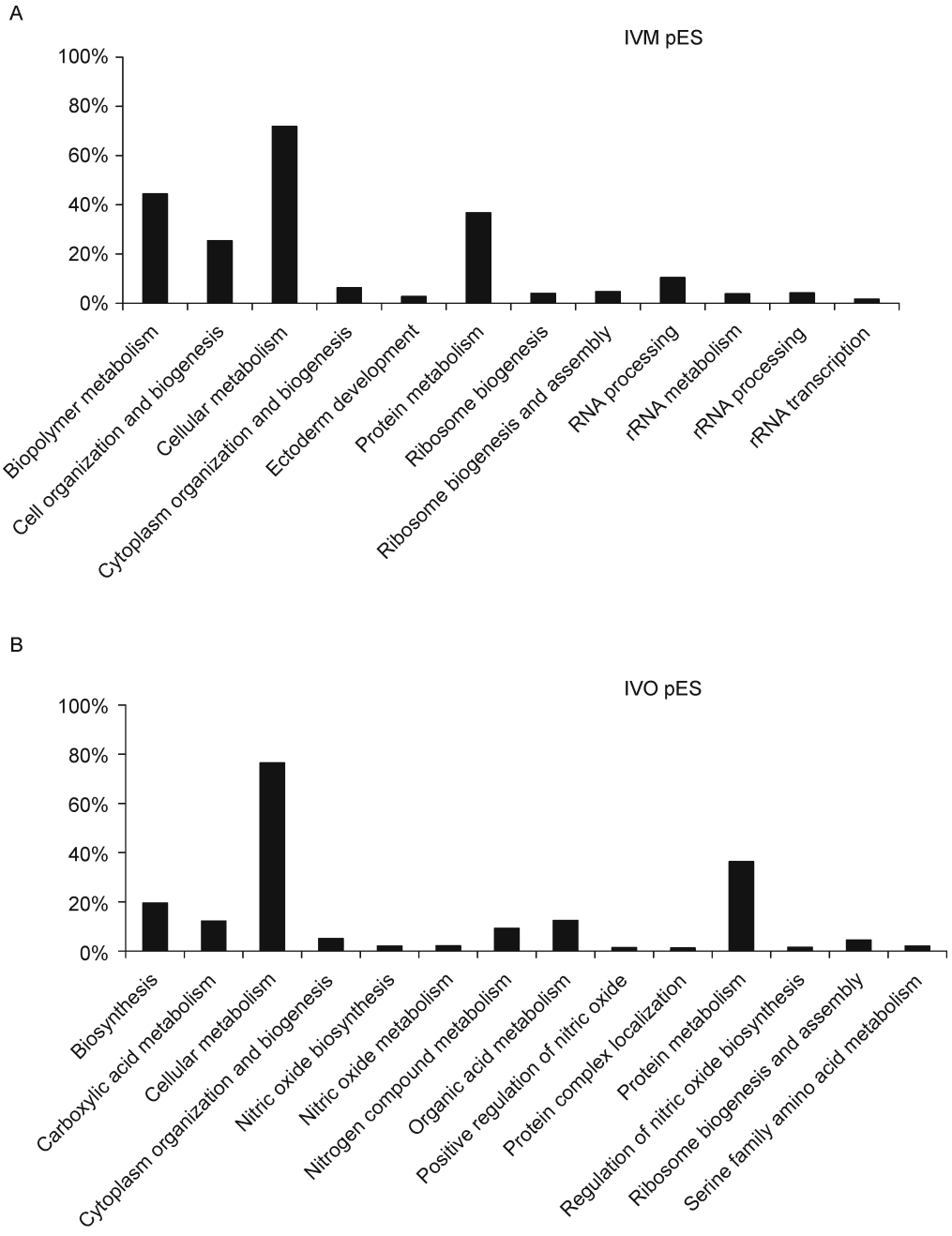

Figure 5. Annotation of the identified proteins and classification according to biological function using the Panther classification system. (A) Ratio of the differentially expressed proteins annotated at the indicated biological process based on all varied proteins in IVM pES cells to those in fES cells. (B) Ratio of the differentially expressed proteins annotated at the indicated biological process based on all varied proteins in IVO pES cells to those in fES cells.

involved in ectoderm and germ cell development, were expressed more in IVM pES cells than in IVO pES cells.

DISCUSSION

The differentially expressed proteins between fES and pES cells were analyzed using two complementary proteomic approaches. Approximately 1300–1500 protein spots were displayed in the DIGE gels, with consistent reproducibility for each sample despite the limited detection of the differentially expressed spots using this technique. Compared to the ICAT data, several low-abundance, hydrophobic, very large, or very small proteins were lost during the DIGE processes. Presumably, low- or high-abundance proteins cannot be

displayed in a single gel, hydrophobic proteins were precipitated during IEF, and small proteins may have run out of the gel (Rabilloud, 2002; Marouga et al., 2005). Using the gel-free proteomics method ICAT (Moseley, 2001), more than 4000 pairs of ICAT-labeled peptides were detected in each ICAT experiment. Over 90 differentially expressed proteins were identified in the two types of pES cells, of which five were in IVM pES and eight in IVO pES, as shown by both ICAT and DIGE results. ICAT sensitivity is superior to that of DIGE. The differential expression of several proteins, such as stathmin 1, annexin A3, annexin A5, prohibitin, glutathione S-transferase, and superoxide dismutase (Cui et al., 2011), between the fES and pES cells as detected by the 2DE method, was also confirmed in the comparison of fES and IVO pES cells using the DIGE method. Apparently, neither ICAT nor DIGE provides a comprehensive coverage on a proteome-wide scale (Aebersold et al., 2000; Wu et al., 2006). ICAT may lose some proteins that do not contain cysteine (Gygi et al., 1999), and may not easily detect modified proteins or protein isoforms generated via alternative splicing (Haynes and Yates, 2000; Zhang et al., 2001). Thus, these two complementary proteomic methods were used in an attempt to identify the differentially expressed proteins in pES and fES cells.

Proteomic analysis shows that more than 5000 distinct proteins were identified in mouse ES cells (Graumann et al., 2008). Among those identified using ICAT and DIGE methods, only 15 showed changes in the expression above 2-fold in IVM pES cells and 29 in IVO pES cells. Thus, the variation in the proteome in pES cells did not significantly differ from that of fES cells. Moreover, IVM pES cell proteome exhibited greater similarity to that of fES than did IVO pES cells. Coincidentally, both types of pES cells exhibited developmental pluripotency, and IVM pES cells showed higher pluripotency, similar to fES cells (Chen et al., 2009; Liu et al., 2011).

Consistently, the expression of the imprinted genes was found relatively normal in both pES cell types, suggesting that the paternally expressed imprinted genes are activated and resemble those of fES cells, which is consistent with the real-time PCR results (Li et al., 2009). More than 80 imprinted genes have been identified (Vigé et al., 2006; Sritanaudomchai et al., 2010), but some are non-coding RNAs that cannot be translated into proteins (Sapienza, 2002; Bartolomei, 2003). In addition, arginine N-methyltransferase 7 was upregulated in both types of pES cells and histone deacetylase 1 was upregulated in the IVO pES cells, suggesting that epigenetic modification may contribute to pES cell reprogramming.

Proteins involved in cellular metabolism, protein metabolism, cytoplasm organization and biogenesis, and ribosome biogenesis were upregulated in both types of pES cells. Hypomethylation underlies the reactivation of the imprinted genes in pES cells (Li et al., 2009), which can result in active RNA transcription and protein synthesis. The increased level of proteins related to oxidation-reduction and apoptosis likely resulted from the *in vitro* isolation and culture conditioning of pES cell lines. Among the differentially expressed proteins in IVM or IVO pES cells, caldesmon 1 was highly expressed in IVM pES cells compared with that in fES cells. Caldesmon is a calmodulin-binding protein that inhibits ATPase activity of myosin in smooth muscle (Huber, 1998) and is upregulated during differentiation of adult stem cells into smooth muscle (Harris et al., 2011). Prdx4, FBP1, the nuclear matrix protein senescence evasion factor (SNEV), and stomatin-like protein 2 were upregulated in IVO pES cells. Prdx4 is an important protective antioxidant enzyme as well as a modulator of hydrogen peroxide-mediated signaling and plays a role in gamete maturation and during embryogenesis (Donnay and Knoops, 2007). FBP1 is usually expressed in undifferentiated cells and is involved in cell growth, proliferation, differentiation, and apoptosis (He et al., 2000). SNEV is very important for early mouse development (Fortschegger et al., 2007). Stomatin-like protein 2 is also involved in regulating cell growth and adhesion. The function of the preferential expression of these proteins in IVM pES or IVO pES cells remains to be elucidated.

Notably, several proteins, such as nestin and the BPY2-interacting protein 1, which are required for embryonic development, were highly expressed only in IVM pES cells. Nestin is a marker for the ectoderm and plays a role in nerve development (Zimmerman et al., 1994); this protein has also been identified in mouse pES cells generated from growing oocytes (Shao et al., 2007). BPY2-interacting protein 1 interacts with ubiquitin protein ligase E3A (Wong et al., 2002) and may be involved in male germ cell development and male fertility. BPY2 (Choi et al., 2007), which encodes BPY2-interacting protein 1, is located in the non-recombinant portion of the Y chromosome and is specifically expressed in the testis (Skaletsky et al., 2003). Whether preferential expression of BPY2 contributes to the high germline competence of IVM pES cells remains to be determined (Liu et al., 2011).

A comparison of the pES and fES cellular peptide sequence data generated by DIGE and ICAT was documented. These global comparisons of protein profiling can be useful in understanding the mechanism underlying the pluripotency of pES cells and may serve as a reference map for future studies and the potential application of pES cells for stem cell therapy.

MATERIALS AND METHODS

IVM parthenogenetic stem cell line

The method used to derive the IVM pES cell lines was as previously described (Liu et al., 2011). Briefly, the cumulus-oocyte-complexes (COCs) at the germinal vesicle stage were collected from

hormone-primed mice by puncturing follicles in 20 mmol/L Hepes-buffered IVM medium. The COCs were cultured in 100 μL droplets of IVM medium and covered with mineral oil at 37°C in 6.5% CO_2 humidified air for 15–16 h until the IVM oocytes reached the metaphase II (MII) stage. The IVM medium consisted of 95% minimum essential medium (MEM, Invitrogen), 5% fetal bovine serum (FBS, Hyclone), 0.24 mmol/L sodium pyruvate, 1.5 IU/mL human chorionic gonadotrophin (hCG), and 1 IU/mL pregnant mare serum gonadotropin (PMSG). Parthenogenetic 'embryos' were produced via the activation of oocytes using $SrCl_2$ and cytochalasin D. The embryos were cultured in 50 μL droplets of potassium simplex optimized medium ($KSOM_{AA}$) and then covered with mineral oil at 37°C in 6.5% CO_2 humidified air. IVM parthenogenetic blastocysts were obtained via culture of the activated IVM MII oocytes for 96 h. Approximately 10 days after IVM blastocyst seeding, the ICM outgrowths were mechanically removed, separated into small clumps, and reseeded on fresh feeder cells. Stable embryonic stem-like (ES) cells were routinely obtained after two or three passages. IVM pESC lines were passaged and cultured in ESC medium supplemented with FBS.

Cell culture and protein extraction

The fES (F1), IVM pES (1116), and IVO pES (C3) cell lines used in the current study were established in the laboratory and were previously reported (Chen et al., 2009; Liu et al., 2011). Chimeras were generated from both pES cell lines 1116 and C3, but IVM pES 1116 chimeras showed high germline transmission. Cell lines grown on mouse embryonic fibroblasts (MEF) were treated with trypsin/EDTA and resuspended in an ESC medium. The mixture was then placed twice on 0.1% gelatin-coated dishes for 30 min to allow MEF to attach to the bottom of the dishes. Cells that remained in the supernate were harvested via centrifugation for 5 min at 1000 rpm and washing with PBS three times. The cells were then stored at −80°C. The cell pellets were lysed via sonication (5 × 10 s pulses on ice) in a sample buffer (7 mol/L urea, 2 mol/L thiourea, 4% CHAPS, and 2% IPG buffer) at a 1:20 *w*/*v* ratio. After centrifugation at 14,000 rpm for 1 h, the protein concentration was determined using the Bio-Rad Protein Assay (Bio-Rad, Hercules, CA) (Bradford, 1976).

DIGE, quantitative spot analysis, and identification of differentially expressed proteins

Stock cyanine dyes (1 nmol/μL) were diluted in anhydrous dimethyl formamide (DMF) p.a. to 400 pmol/μL (GE Healthcare). The dye (400 pmol per 50 μg protein) was added to the cell lysate. The sample was vortexed, briefly centrifuged, and left on ice for 30 min in the dark. The labeling reaction was stopped by adding 10 mmol/L L-lysine (1 μL per 400 pmol dye). After vortexing and centrifugation, the sample was left on ice for 10 min in the dark. Proteins extracted from the stem cells were labeled with Cy3 or Cy5 (Supplementary Table S1), mixed with Cy2-labeled internal standards, and run in one gel. The internal standard contained equivalent amounts of pooled proteins, including four samples which proved useful for internal calibration purposes.

Exactly 100 μL of pooled Cy3- or Cy5-labeled proteins was mixed with 2D DIGE buffer (8 mol/L urea, 2% CHAPS, 18 mmol/L DTT, 0.5% IPG buffer) and used for isoelectric focusing (IEF); IEF was performed on 13 cm IPG strips (PH3-10, NL), and the focusing parameters were initiated as follows: 30 V, rehydration for 12 h, 500 V for 1 h, 1000 V for 1 h, then 8000 V until a total of 48,000 V h was reached, and then hold at 500 V. The strips were equilibrated in 6 mol/L urea, 2% SDS, 50 mmol/L Tris-HCl, pH 8.8, 20% *v*/*v* glycerol, and 2% DTT for 15 min, and then placed in the same buffer for another 15 min, except that DTT was replaced with 2.5% iodoacetamide. The strips were placed onto the stacking gel without an agarose plug.

2-DE was performed using 12.5% SDS-PAGE gels at 15 mA per gel for 30 min, and then at 30 mA per gel until the bromophenol blue front reached the end of the IPG strip. Cy3- and Cy5-labeled images were acquired using a Typhoon 9400 scanner (GE Healthcare).

The SDS-PAGE gels were scanned using a Typhoon 9400 scanner (Amersham Biosciences). The excitation and emission wavelengths were specifically chosen for each of the dyes according to the recommendations of the manufacturer. The images were preprocessed using the ImageQuantTM software (Amersham Biosciences). Intra-gel spot detection and inter-gel matching were performed using the differential in-gel analysis (DIA) and biological variation analysis (BVA) modes of the DeCyder software (Amersham Biosciences), respectively. The spot intensities were normalized to the internal standard and the significantly regulated proteins were identified using the Student's *t*-test. The differentially expressed protein spots ($p < 0.05$) between either IVO pES or IVM pES and fES were identified using MS.

Preparative IEF was performed by increasing the protein amount loaded onto the IPG strips for spot picking. Exactly 1 mg protein was used for 2D electrophoresis, which was performed as previously described. After SDS-PAGE, the gel was stained with Coomassie brilliant blue according to the manufacturer's instructions.

Spots of interest were manually cut out of the preparative gel, digested in-gel with trypsin (Promega, Madison, WI), and extracted from the gel. Briefly, specific protein spots were washed twice with 30% acetonitrile (ACN) in 100 mmol/L ammonium bicarbonate (NH_4HCO_3) and vacuum-dried. The gel samples were then reduced with DTT (10 μL 100 mmol/L NH_4HCO_3, 56°C for 0.5 h) and alkylated using iodoacetamide (60 mmol/L in 100 mmol/L NH_4HCO_3, room temperature for 35 min). Next, the gel pieces were vacuum-dried, rehydrated in 5 μL digestion buffer (10 ng/μL trypsin in 100 mmol/L NH_4HCO_3), and covered with a minimum volume of NH_4HCO_3. After overnight digestion at 37°C, the peptides were extracted three times with a solution containing 60% ACN and 0.1% formic acid. The extracted digests were vacuum-dried.

C18 ZipTips™ (Millipore, Bedford, MA) were used for the MALDI target preparation. The peptides were eluted on the MALDI target with 2 μL matrix solution [α-cyano-4-hydroxy cynnamic acid in ACN and 0.1% trifluoroacetic acid (TFA, 1:1, *v*/*v*)]. For tryptic peptide analysis, MALDI-TOF MS was performed using the UltraFlex TOF-TOF LIFT MS (Bruker Daltonik, Bremen, Germany). The spectra were acquired in the positive mode, with a target voltage of 20 kV and the reflector voltage at 23 kV. The internal calibration of the peptide mass fingerprinting (PMF) spectra was performed using the autolysis products of trypsin with the monoisotopic masses m/z = 842.51, 1045.5642, and 2211.1046 Da. The PMF spectra were processed using the Mascot search engine to identify the proteins.

ICAT labeling, quantitative analysis, and identification of differentially expressed peptides

Protein samples were reconstituted with the labeling buffer supplied with the ICAT Reagent Kit (ABI) and processed according to the

manufacturer's protocol. Protein samples (200 μg) from each fES were separately labeled with the heavy ICAT reagent, whereas those from a paired control group (IVM pES and IVO pES) were labeled with the light ICAT reagent. The labeling process was conducted in denaturing buffer [50 mmol/L Tris-HCl, pH 8.5, 0.1% SDS, and 1 mmol/L tris(2-carboxyethyl)phosphine (TCEP)]. Each heavy ICAT-labeled sample was mixed with the light ICAT-labeled pooled control sample and digested with 30 μg trypsin (Promega, Madison WI) at 37°C for 16 h. The resulting peptides were purified on cation exchange and avidin cartridges (Applied Biosystems) and subsequently incubated with cleaving reagents A and B (Applied Biosystems) in a 95:5 ratio (100 μL total volume) according to the manufacturer's protocol.

Each peptide fraction was analyzed via LC-MS/MS using a Thermo LTQ linear trap MS (Thermo Electron Corporation, San Jose, CA) equipped with a Thermo microelectrospray source. An online RP LC column (100 mm × 180 μm i.d., PepMap C18) was used for all analyses. The peptides were sequentially eluted with a 0%–100% gradient of buffer B (ACN:water:acetic acid, 80:9.9:0.1) in buffer A (ACN:water:acetic acid, 5:94.9:0.1) for 180 min at a post-split flow rate of 100 nL/min. The electrospray source parameters were 2.25 kV electrospray voltage, 5 V capillary voltage, 400–2000 m/z range, and 35% normalized MS/MS collision energy. Data were analyzed using Bioworks and Qual Brower.

Real-time PCR

Total RNA was extracted from ES cells using RNeasy Micro Kit according to the manufacturer's instructions. Extracted RNA was subjected to cDNA synthesis using QuantiTect Reserve Transcription (Qiagen). GAPDH served as a reference control and was corrected for PCR efficiency in differences between target and reference with efficiency correction using Relative Quantification Software (Roche LC 480). Standard curves were prepared for each gene using known quantities of total cDNA from other cells. Thermal cycling was conducted with a 10 min denaturation step at 94°C, followed by 40 three-step cycles: 30 s at 94°C, 30 s at 56°C or 58°C, and 30 s at 72°C. Primers for the real-time PCR are listed in detail in Table S2.

ACKNOWLEDGEMENTS

This work was supported by MOST National Major Basic Research Program (Grant Nos. 2010CB94500, 2009CB941000 (to LL), and 2010CB833703 (to FY)).

ABBREVIATIONS

DIGE, fluorescent two-dimensional difference in-gel electrophoresis; fES, fertilized embryonic stem cells; ICAT, isotope-coded affinity tag; IEF, isoelectric focusing; IVM, *in vitro* maturation; IVO, *in vivo* ovulated; MALDI-TOF, matrix-assisted laser desorption/ionization time-of-flight mass spectrometry; MEF, mouse embryonic fibroblast; PCR, polymerase chain reaction; pES, parthenogenetic embryonic stem cells

Supplementary material is available in the online version of this article at http://dx.doi.org/10.1007/s13238-011-1081-7 and is accessible for authorized users.

REFERENCES

Aebersold, R., Rist, B., and Gygi, S.P. (2000). Quantitative proteome analysis: methods and applications. Ann N Y Acad Sci 919, 33–47.

Bartolomei, M.S. (2003). Epigenetics: role of germ cell imprinting. Adv Exp Med Biol 518, 239–245.

Bradford, M.M. (1976). A rapid and sensitive method for the quantitation of microgram quantities of protein utilizing the principle of protein-dye binding. Anal Biochem 72, 248–254.

Brevini, T.A., and Gandolfi, F. (2008). Parthenotes as a source of embryonic stem cells. Cell Prolif 41, 20–30.

Chen, Z., Liu, Z., Huang, J., Amano, T., Li, C., Cao, S., Wu, C., Liu, B., Zhou, L., Carter, M.G., *et al.* (2009). Birth of parthenote mice directly from parthenogenetic embryonic stem cells. Stem Cells 27, 2136–2145.

Choi, J., Koh, E., Suzuki, H., Maeda, Y., Yoshida, A., and Namiki, M. (2007). Alu sequence variants of the BPY2 gene in proven fertile and infertile men with Sertoli cell-only phenotype. Int J Urol 14, 431–435.

Cibelli, J.B., Grant, K.A., Chapman, K.B., Cunniff, K., Worst, T., Green, H.L., Walker, S.J., Gutin, P.H., Vilner, L., Tabar, V., *et al.* (2002). Parthenogenetic stem cells in nonhuman primates. Science 295, 819.

Cui, X.S., Shen X.H., Lee, C.K., Kang, Y.K., Wakayama, T., and Kim N.H. (2011). Analysis of proteomic profiling of mouse embryonic stem cells derived from fertilized, parthenogenetic and androgenetic blastocysts. Stem Cell Discovery 1, 1–15.

De Sousa, P. A., and Wilmut, I. (2007). Human parthenogenetic embryo stem cells: appreciating what you have when you have it. Cell Stem Cell 1, 243–244.

Dighe, V., Clepper, L., Pedersen, D., Byrne, J., Ferguson, B., Gokhale, S., Penedo, M.C., Wolf, D., and Mitalipov, S. (2008). Heterozygous embryonic stem cell lines derived from nonhuman primate parthenotes. Stem Cells 26, 756–766.

Donnay, I., and Knoops, B. (2007). Peroxiredoxins in gametogenesis and embryo development. Subcell Biochem 44, 345–355.

Fang, Z.F., Gai, H., Huang, Y.Z., Li, S.G., Chen, X.J., Shi, J.J., Wu, L., Liu, A., Xu, P., and Sheng, H.Z. (2006). Rabbit embryonic stem cell lines derived from fertilized, parthenogenetic or somatic cell nuclear transfer embryos. Exp Cell Res 312, 3669–3682.

Fortschegger, K., Wagner, B., Voglauer, R., Katinger, H., Sibilia, M., and Grillari, J. (2007). Early embryonic lethality of mice lacking the essential protein SNEV. Mol Cell Biol 27, 3123–3130.

Graumann, J., Hubner, N.C., Kim, J.B., Ko, K., Moser, M., Kumar, C., Cox, J., Schöler, H., and Mann, M. (2008). Stable isotope labeling by amino acids in cell culture (SILAC) and proteome quantitation of mouse embryonic stem cells to a depth of 5,111 proteins. Mol Cell Proteomics 7, 672–683.

Gygi, S.P., Rist, B., Gerber, S.A., Turecek, F., Gelb, M.H., and Aebersold, R. (1999). Quantitative analysis of complex protein mixtures using isotope-coded affinity tags. Nat Biotechnol 17, 994–999.

Harris, L.J., Abdollahi, H., Zhang, P., McIlhenny, S., Tulenko, T.N., and DiMuzio, P.J. (2011). Differentiation of adult stem cells into smooth muscle for vascular tissue engineering. J Surg Res 168, 306–314.

Haynes, P.A., and Yates, J.R. 3rd. (2000). Proteome profiling-pitfalls and progress. Yeast 17, 81–87.

He, L., Liu, J., Collins, I., Sanford, S., O'Connell, B., Benham, C.J., and Levens, D. (2000). Loss of FBP function arrests cellular proliferation and extinguishes c-myc expression. EMBO J 19, 1034–1044.

Horii, T., Kimura, M., Morita, S., Nagao, Y., and Hatada, I. (2008). Loss of genomic imprinting in mouse parthenogenetic embryonic stem cells. Stem Cells 26, 79–88.

Huber, P.A. (1998). Caldesmon. Int J Biochem Cell Biol 29, 1047–1051.

Jiang, H., Sun, B., Wang, W., Zhang, Z., Gao, F., Shi, G., Cui, B., Kong, X., He, Z., Ding, X., *et al.* (2007). Activation of paternally expressed imprinted genes in newly derived germline-competent mouse parthenogenetic embryonic stem cell lines. Cell Res 17, 792–803.

Kim, K., Lerou, P., Yabuuchi, A., Lengerke, C., Ng, K., West, J., Kirby, A., Daly, M.J., and Daley, G.Q. (2007). Histocompatible embryonic stem cells by parthenogenesis. Science 315, 482–486.

Levchenko, A. (2005). Proteomics takes stem cell analyses to another level. Nat Biotechnol 23, 828–830.

Li, C., Chen, Z., Liu, Z., Huang, J., Zhang, W., Zhou, L., Keefe, D.L., and Liu, L. (2009). Correlation of expression and methylation of imprinted genes with pluripotency of parthenogenetic embryonic stem cells. Hum Mol Genet 18, 2177–2187.

Liu, Z., Hu, Z., Pan, X., Li, M., Togun, T.A., Tuck, D., Pelizzola, M., Huang, J., Ye, X., Yin, Y., *et al.* (2011). Germline competency of parthenogenetic embryonic stem cells from immature oocytes of adult mouse ovary. Hum Mol Genet 20, 1339–1352.

Lyakhovich, A., Canals, F., Nosov, M., and Surralles, J. (2007). A DIGE-based approach to study interacting proteins. J Biochem Biophys Methods 70, 693–695.

Mai, Q., Yu, Y., Li, T., Wang, L., Chen, M.J., Huang, S.Z., Zhou, C., and Zhou, Q. (2007). Derivation of human embryonic stem cell lines from parthenogenetic blastocysts. Cell Res 17, 1008–1019.

Mann, J.R., Gadi, I., Harbison, M.L., Abbondanzo, S.J., and Stewart, C.L. (1990). Androgenetic mouse embryonic stem cells are pluripotent and cause skeletal defects in chimeras: implications for genetic imprinting. Cell 62, 251–260.

Marouga, R., David, S., and Hawkins, E. (2005). The development of the DIGE system: 2D fluorescence difference gel analysis technology. Anal Bioanal Chem 382, 669–678.

Monk, M. (1988). Genomic imprinting. Genes Dev 2, 921–925.

Moseley, M.A. (2001). Current trends in differential expression proteomics: isotopically coded tags. Trends Biotechnol 19, S10–S16.

Nagano, K., Taoka, M., Yamauchi, Y., Itagaki, C., Shinkawa, T., Nunomura, K., Okamura, N., Takahashi, N., Izumi, T., and Isobe, T. (2005). Large-scale identification of proteins expressed in mouse embryonic stem cells. Proteomics 5, 1346–1361.

Rabilloud, T. (2002). Two-dimensional gel electrophoresis in proteomics: old, old fashioned, but it still climbs up the mountains. Proteomics 2, 3–10.

Sapienza, C. (2002). Imprinted gene expression, transplantation medicine, and the "other" human embryonic stem cell. Proc Natl Acad Sci U S A 99, 10243–10245.

Shao, H., Wei, Z., Wang, L., Wen, L., Duan, B., Mang, L., and Bou, S. (2007). Generation and characterization of mouse parthenogenetic embryonic stem cells containing genomes from non-growing and fully grown oocytes. Cell Biol Int 31, 1336–1344.

Skaletsky, H., Kuroda-Kawaguchi, T., Minx, P.J., Cordum, H.S., Hillier, L., Brown, L.G., Repping, S., Pyntikova, T., Ali, J., Bieri, T., *et al.* (2003). The male-specific region of the human Y chromosome is a mosaic of discrete sequence classes. Nature 423, 825–837.

Sritanaudomchai, H., Ma, H., Clepper, L., Gokhale, S., Bogan, R., Hennebold, J., Wolf, D., and Mitalipov, S. (2010). Discovery of a novel imprinted gene by transcriptional analysis of parthenogenetic embryonic stem cells. Hum Reprod 25, 1927–1941.

Surani, M.A. (1998). Imprinting and the initiation of gene silencing in the germ line. Cell 93, 309–312.

Vigé, A., Gallou-Kabani, C., Gross, M.S., Fabre, A., Junien, C., and Jais, J.P. (2006). An oligonucleotide microarray for mouse imprinted genes profiling. Cytogenet Genome Res 113, 253–261.

Wang, D., and Gao, L. (2005). Proteomic analysis of neural differentiation of mouse embryonic stem cells. Proteomics 5, 4414–4426.

Wang, S., Tang, X., Niu, Y., Chen, H., Li, B., Li, T., Zhang, X., Hu, Z., Zhou, Q., and Ji, W. (2007). Generation and characterization of rabbit embryonic stem cells. Stem Cells 25, 481–489.

Wong, E.Y., Tse, J.Y., Yao, K.M., Tam, P.C., and Yeung, W.S. (2002). VCY2 protein interacts with the HECT domain of ubiquitin-protein ligase E3A. Biochem Biophys Res Commun 296, 1104–1111.

Wu, W.W., Wang, G., Baek, S.J., and Shen, R.F. (2006). Comparative study of three proteomic quantitative methods, DIGE, cICAT, and iTRAQ, using 2D gel- or LC-MALDI TOF/TOF. J Proteome Res 5, 651–658.

Zhang, R., Sioma, C.S., Wang, S., and Regnier, F.E. (2001). Fractionation of isotopically labeled peptides in quantitative proteomics. Anal Chem 73, 5142–5149.

Zimmerman, L., Parr, B., Lendahl, U., Cunningham, M., McKay, R., Gavin, B., Mann, J., Vassileva, G., and McMahon, A. (1994). Independent regulatory elements in the nestin gene direct transgene expression to neural stem cells or muscle precursors. Neuron 12, 11–24.

